1-1-2010

Assessing the long-term urban heat island in San Antonio, Texas based on moderate resolution imaging spectroradiometer/Aqua Data

Hongjie Xie

Ni-Bin Chang
University of Central Florida

Ammarin Daranpob
University of Central Florida

David Prado

Journal of
Applied Remote Sensing

Assessing the long-term urban heat island in San Antonio, Texas based on moderate resolution imaging spectroradiometer/Aqua Data

Hongjie Xie
Ni-Bin Chang
Ammarin Daranpob
David Prado

Assessing the long-term urban heat island in San Antonio, Texas based on moderate resolution imaging spectroradiometer/Aqua Data

Hongjie Xie,[a] Ni-Bin Chang,[b] Ammarin Daranpob,[b] and David Prado[a]

[a] University of Texas at San Antonio, Department of Geological Science, Laboratory for Remote Sensing and Geoinformatics, San Antonio, TX, USA
Hongjie.Xie@utsa.edu

[b] University of Central Florida, Civil, Environmental, and Construction Engineering Department, Orlando FL, USA
nchang@mail.ucf.edu and ammarin_r@hotmail.com

Abstract. Urban environmental conditions are strongly dependent on the land use and land cover properties. Urban and rural areas normally exhibit obvious difference in land surface temperature (LST). The Moderate Resolution Imaging Spectroradiometer (MODIS) Aqua (PM satellite) MYD11A1 temperature products (daily and 1 km spatial resolution) for the period from June 1 to September 30 between 2002 and 2008 were used to screen the existence of urban heat island (UHI) phenomena for the city of San Antonio, TX. 8-day MYD11A2 temperature products between 2002 and 2008 were also retrieved to map the temperature climatology at the 1:30 a.m. for the region. The UHI effect was detected in both satellite surface-temperature and meteorological station air-temperature record. The existence of an UHI of the San Antonio downtown area was clearly shown in about 90% of the available cloud-free (or cloudless) data from June 1-September 30 each year. It is especially prevalent in the night-time imagery due to less cloud contamination. During nighttime, the heat island (HI) is about 4 - 5 °K (6 - 8 °F) higher than the average temperature of the study area and 6 - 7 °K (8 - 12 °F) higher than the rural area. Surprisingly, the HI phenomenon is found not only in the downtown area, but also several other small areas in the northern corner. Finally, the long-term UHI effect of San Antonio and its relationship with normalized difference vegetation index (NDVI) were discussed. USGS rainfall data were also used to discuss the possible connections between the UHI and several local storm events.

Keywords: Heat island; Land surface temperature, MODIS.

1 INTRODUCTION

Urbanization has driven extensive modifications of land use and land cover in urban region for domestic, commercial, and industrial uses, contributing to changes in the hydrologic cycle and increased pollution at different temporal and spatial scales. Urban heat island (UHI) phenomenon is due to increased local atmospheric and surface temperatures in urban areas compared to the surrounding rural areas [1]. The UHIs can perhaps be taken as harbingers of the effect of global climate change because they could affect not only local and regional climate to some extent, but also hydrological cycle, air quality, human health, biodiversity, and ecosystem functioning. These results are mainly due to the concentration of human activities and artificial land uses such as dense transportation network, buildings and parking lots.

 [DOI: 10.1117/1.3335611]
Received 15 Jul 2009; accepted 3 Feb 2010; published 6 Feb 2010 [CCC: 19313195/2010/$25.00]

Several attempts to describe the complex UHIs have been made over the past decade trying to bring up a consistent picture of the causal effect of the UHIs. For example, they might be tied with urban air pollution, especially ozone concentration because of its sensitivity to air temperature, electric power consumption, and airport operation. A previous study [2] using air temperature measurement from 1946 to 1990 has shown that San Antonio has an increased UHI effect. On the other hand, in June 18, 2000, NASA reported that the TRMM rainfall data confirm the summer rainfall increase over the San Antonio area, due to the UHI effect [3]. They found that urban areas with high densities of buildings, roads and other artificial surfaces retain heat and lead to warmer surrounding temperatures, and create urban heat-islands. This increased heat may promote rising air and alter the weather around cities [3]. Within a four-city survey, including Atlanta, Dallas, San Antonio and Nashville, mean monthly rainfall rates within 30-60 kilometers (18 to 36 miles) downwind of the cities were, on average, about 28 percent greater than the upwind region. In some cities, the downwind area exhibited increases as high as 51 percent [2]. The hypothesis was that the added heat creates wind circulations and rising air that can produce clouds or enhance existing ones mostly during the warmer months and these clouds can evolve into rain-producers or storms under the right conditions [2].

Land surface temperatures (LST) derived from both Landsat and Moderate Resolution Imaging Spectroradiometer (MODIS) thermal images were analyzed as a surrogate index of UHI for spatial patterns of heat islands in Europe, the US and China [4][5]. Chudnovsky et al. [6] suggested that the best remote sensing for urban heat environment study should be conducted twice: in the early before sunrise (5 a.m.) and in the early noon hours (12-1 p.m.). The satellite based thermal remote sensing technology that can produce the LST information make it possible to study the UHI both remotely and on continental or global scale because of a positive correlation with between surface temperature and air temperature [7]. It is known that flow distortion, topography, and roughness effect can result in differences between urban air temperature and LST [8]. The UHI is actually a phenomena linked with the urban air temperature directly [9]. Meteorological simulations with use of satellite data for assessing urban heat island under summertime anticyclonic conditions was considered to account for local disparity between LST and urban air temperature [9]-[11]. LST derived from LANDSAT and AVHRR thermal bands were used for the UHI studies [12]-[14]. Many cities in Texas have urban districts with low element height and density or more densely built-up districts with relatively uniform element height and density (buildings and trees). It is believed that the use of LST to replace urban air temperature for conducting the UHI assessment is not overly compromised due to the presence of widely dispersed open grass land in these cities such as Dallas, Houston, San Antonio, El Paso, etc. Thus, this paper aims to examine a series of LST data with different temporal scales to delineate the UHI effect in a seven-year time frame. For the purpose of clarity, the term, UHI, used in this paper stands actually for Surface Urban Heat Island (SUHI) that is a surrogate index for addressing the heat island effect indirectly.

In addition to the heat wave received due to the UHI effect, urban environmental conditions are strongly dependent on the land use properties and radiant thermal field of the land cover elements in the urban mosaic. Observations of urban emissivity and LST provide valuable constraints on the biophysical properties that might become the determinants of the UHI formation. Further, the added heat could create local wind circulations and rising air that can produce clouds or enhance existing ones mostly during the warmer months. These clouds in turn can be affected by the changes of climate patterns under global climate change impacts, which is called "country breeze" in the urban climate domain [3][4]. Final extended discussion of this paper touches the base of sing simple ratio for addressing possible linkages between the UHI and the normalized difference vegetation index (NDVI) on one hand, and explaining the possible connections between the UHI and the urban storm events on the other hand.

2 THE STUDY AREA

Figure 1 shows the study area of the City of San Antonio, Texas and its surrounding area (~14,221 km^2). San Antonio is located in south central Texas between the Edwards Plateau to the northwest and the Gulf Coastal Plains to the southeast. From the central area of the city to the rural areas, it includes three loops geographically, namely loop 410, loop 1604, and a rural loop. The San Antonio metropolitan area has about 1.5 million people, which is ranked the 8^{th} largest city of the nation. San Antonio possesses a modified subtropical climate. Its average annual rainfall is 697 mm (27.45 inches) per year and average temperature is 21°C (69.9°F). May and September oftentimes receive the most rainfall building to thunderstorms with winds from the southeast. The city's proximity to the Gulf of Mexico can bring San Antonio some severe tropical storms resulting in flash flood in urban regions.

Two river systems as seen in Fig. 1 are San Antonio River passing through the San Antonio downtown area and Guadalupe River in the northeastern portion of the study area. Both river systems flow southeast towards the Gulf of Mexico. There are several water bodies (lakes) in the area. The largest fours are Canyon Lake, Medina Lake, Calaveras Lake, and Braunic Lake. There are several small to middle size towns and cities around the San Antonio metropolitan area, such as the New Braunfels and Seguin. Figure 2 is a production of digital elevation model (DEM) showing the study area with elevation gradients. Obviously, the altitude of this area declines from northwest to southeast from over 600 m to less than 100 m above the sea level. The City of San Antonio is between 130 to 330 m with an average of 216 m above the sea level. Basically, the northwest portion of the area (just outside of the city limit) is part of the Texas Hill Country. The present landscape of this Hill Country area is dominated by mostly forest and rangeland. Yet other areas (other than the Hill Country) are mainly agricultural, which can be easily differentiated by the isolated forest patches and rangeland using the LANDSAT-ETM+ image as shown in Fig. 1.

3 MATERIALS AND METHODS

3.1 MODIS Data

MODIS is a remote sensing instrument on board space-borne satellites Terra and Aqua launched in February 2000 and May 2002, respectively. Its images provide tremendous environmental and geophysical data of globe coverage in four times per day with good spatial resolution from 250 m to 1 km [17]. Terra travels from north to south across the equator in the morning (10:30 am), whereas Aqua travels from south to north over the equator in the afternoon (1:30 pm). The two satellites can view the whole earth's surface once in every 1-2 days. MODIS can acquire electromagnetic energy via 36 spectral bands. The data are used to observe and improve understanding of changes at and above the earth's surface. Spatial resolution of MODIS images include 250 m (bands 1-2), 500 m (bands 3-7), and 1000 m (bands 8-36). Of the many products the MODIS instrument provides, the most common one is the daily or 8-day 1 km spatial resolution of LST and emissivity with high accuracy of 1 °K [18]-[19]. Time periods used for this study are daily data (MYD11A1) from June 1 to September 30 between 2002 and 2008 as well as 8-day data (MYD11A2) between 2002 and 2008. All products were ordered through EOS Data Gateway [17].

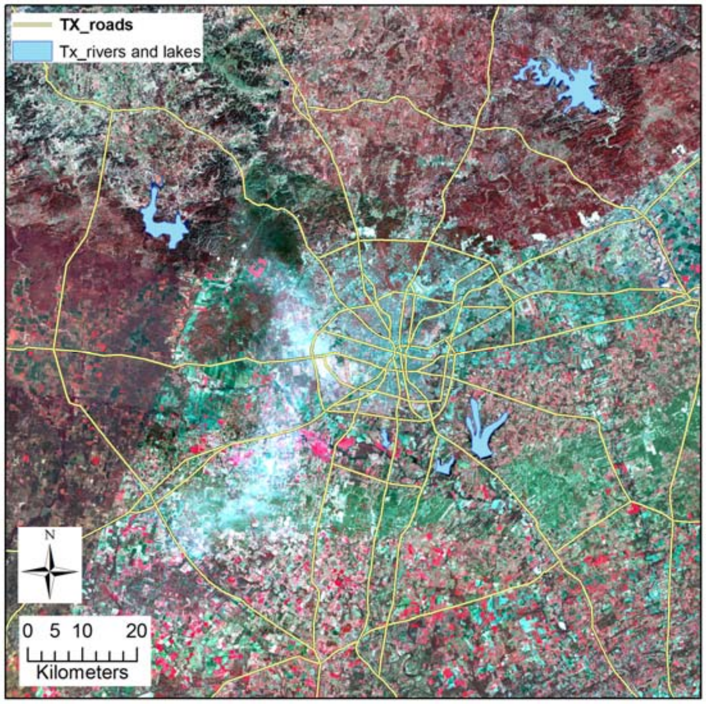

Fig. 1. The study area shown by the river systems and major roads overlaying on a portion of four maosaicked Landsat ETM+.

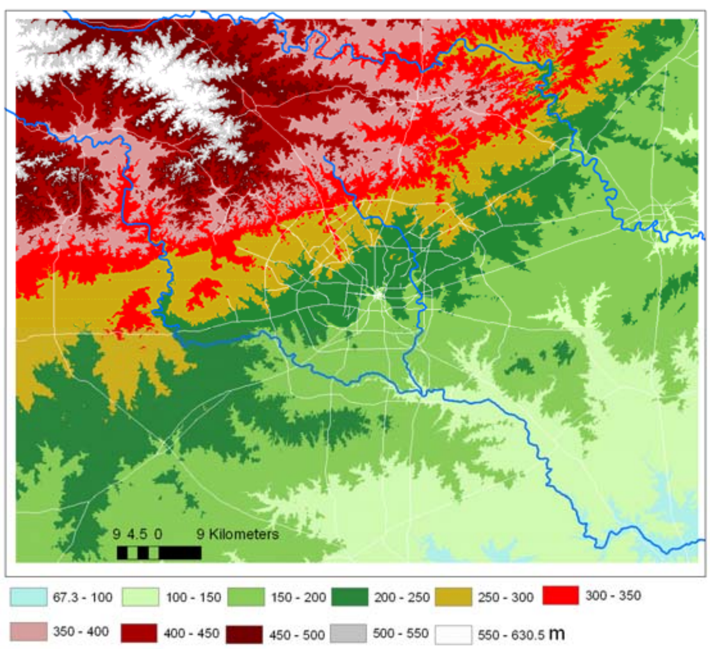

Fig. 2. The study area and the elevation gradients.

3.2 Data of Land Surface Temperature

A developed batch model of MODIS Re-projection Tool (MRT tool) was used to automatically process all seven-year data based on the following steps: (1) select night time and day time LST images, (2) clip the images to study area and (3) reproject the clipped images to UTM zone 14 with WGS84 datum [18]. Using Erdas Imagine® (e.g., an image processing software), the time series of images were stacked into two images: daytime image and nighttime image. These two stacked images were then converted to real temperature (Kelvin) by multiply the scale factor of 0.02. This method also allows for a measurement of the overall spatial breadth of the UHI. Because of the presence of cloud contamination, MODIS only retrieves the data of day's and night's temperature and emissivity using a cloud mask during clear sky (MOD35, another MODIS product) [19]. Every LST map associated with the two stacked images was subjected for visual check to examine the cloud-induced contamination. Basically, if contaminated by cloud, the image will leave a hole with no data, and this data may not be used for further analysis. For example, the following image of day 216 in 2004 (8/3/2004) as shown in Fig. 3(a) is seriously contaminated by cloud. The black holes have no temperature data. In fact, only about 150 images (both daytime and nighttime) out of the study periods of seven years were found cloud-free and/or near cloud-free. A Delaunay triangulation interpolation method was used to fill the pixels (no data) with triangles calculated from the surrounding good temperature values for those near cloud-free image only. To address the relative changes of LST from downtown to rural areas, a numerical index can be defined as simple ratio, which is denoted as UHI/OHI symbolically. As Fig. 3b shows, the OHI includes the area outside the blue circle and inside the yellow circle (donut shape) whereas the UHI includes the area inside the blue circle. The UHI and OHI temperatures are defined as the averaged temperatures measured within the respectively marked area in the figure, from which the simple ratio can be derived as a temperature ratio of urban/rural measurements. The larger the simple ratio is, the higher the UHI effect.

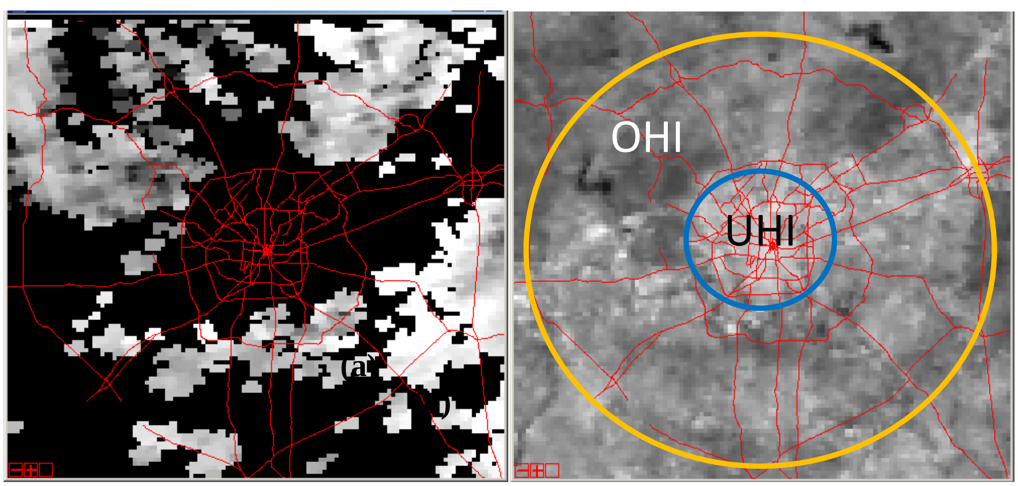

Fig. 3. (a) The MODIS-derived daytime (1:30 pm, CST) LST of day 216 (8/3/2004) with major roads overlaying on it. The black area (pixels) means that there is no temperature data available due to cloud effect detected by the MODIS cloud mask (MOD35). (b) The MODIS-derived daytime LST of day 217 (8/4/2004) with the major roads overlaying on it. The scattered black holes (pixels) where no data are available due to cloud mask have been filled by using Delaunay triangulation method.

3.3 Data of Normalized Difference Vegetation Index

The MODIS NDVI data set is available for the seven year period between 2002 and 2008 [17]. The data products include a temporal resolution of 16-day and one month associated with three nominal spatial resolutions: 250-, 500-, and 1000-meter. The MODIS Aqua product MYD13A1 Vegetation Indices 16-Day L3 500-m was used finally for extended discussion. The data are publicly accessed and can be requested and obtained from the Warehouse Inventory Search Tool (WIST) [17]. The MRT tool was used to convert MYD13A1 in HDF-EOS format to GeoTIFF format, which was then imported to ArcGIS® for visualization and spatial analysis. The range of NDVI data is normally between -1 and 1, where the values from 0 – 0.3 indicate bare soil and rock, and the values greater than 0.3 indicate vegetation greenness.

3.4 Data for Plausible Connections between LST and Urban Storms

The USGS gage station (08178565) at San Antonio River Loop 410 was selected for the collection of rainfall data. This station is located at Latitude 29 19' 19"N and Longitude 98 27' 00"W. The datum of gage is 148 m (488.11 feet) above sea level NGVD29. It drains the runoff from Bexar County, Texas (Hydrologic unit 12100301) with a drainage area of 201.2 square kilometers (125 square miles) [20]. Within the seven-year time frame, screening of the simple ratios associated with storm events would enable us to compare the patterns visually so that drastic variations of the simple ratios may be correlated with the single or multiple peaks of the precipitation. On the other hand, surface emissivity estimation is a significant factor for the LST estimation from remotely sensed data. In eastern part of the US, the emissivity estimation can be performed for fully vegetated surfaces in a simple manner since the emissivity is relatively uniform. However, in the western part of the US, the estimation becomes more complicated for arid land with sparse vegetation since the emissivity of the exposed soil and rock is highly variable. NDVI-based emissivities used to be a critical factor affecting the LST [21].

4 RESULTS AND DISCUSSION

4.1 Urban Heat Island Effect

About 150 good LST images (both daytime and nighttime) for the study periods (June to September) of 2002-2008 have been analyzed. The existence of a UHI of the San Antonio downtown area was clearly shown in ~ 90% of the available cloud-free (or near free) data. It is especially prevalent in the night-time imageries than in the daytime imageries due to less cloud contamination. Overall, during nighttime, the UHI is about 4 - 5 °K (6 - 8 °K) higher than the average temperature of the study area and 6 - 7 °K (8 - 12 °K) higher than the rural area. The temperature difference that is higher in the daytime than in the nighttime is due to the solar radiation which is a added factor to the UHI in the day time, since the added factor is even higher for the urban concrete area (impervious surface) than in the rural area (more pervious surface).

Surprisingly, the UHI phenomenon is found not only in the downtown area, but also several other small areas in the northern corner of city’s urban area in particular at: (1) the area of Loop 410 between San Pedro and San Antonio International Airport and (2) the triangle area among IH-10, Fredericksburg, and Wurzbach. Occasionally, the UHI was also evident outside of the city’s urban area in the day-time imageries. It may be related to both bare/fallow agriculture fields and rainfall events before the image acquisition [15].

Figure 4 is an example of daytime (1:30 p.m., CST) LST in day 153 (6/2/2005). This image clearly shows the UHI of the downtown area (UHI1) and several other small areas, such as, the area at LP410 from San Pedro through HW 281 to Harry Wurzbach HWY (including the North Star Mall and Airport) (UHI2) and the area at the Wurzbach PKWY and Fredericksburg RD (UHI3). To our knowledge, those small UHI areas have never been reported, thereby deserving more detailed studies in the future. The average temperature of each UHI is ~317.5 °K. The rest of Loop 410 area (e.g., not including the south, southeast and southwest portions) has average of 315 °K, which is 2.5 °K lower than the UHI. North and northwest of Loop 1604 area has average temperature of 312 °K, which is 5.5 °K lower than UHI. Rural area in northwest of the study area is ~9.5 °K lower than the UHI, while rural area in southwest is ~7.5 °K lower than the UHI. Water bodies have lower temperature; especially the Canyon Lake has the lowest T ~298 °K, which is about 19.5 °K lower than the UHI. Fig. 5 further shows the difference between summer and winter time comparatively. In Aug. 2007, the UHI turned out to be much more significant and almost most of the urban and northern suburban areas were affected by the UHI. Yet the UHI in winter 2004 appeared to be limited in downtown area and the northwest corner where the University of Texas – San Antonio main campus and the neighboring communities are located at.

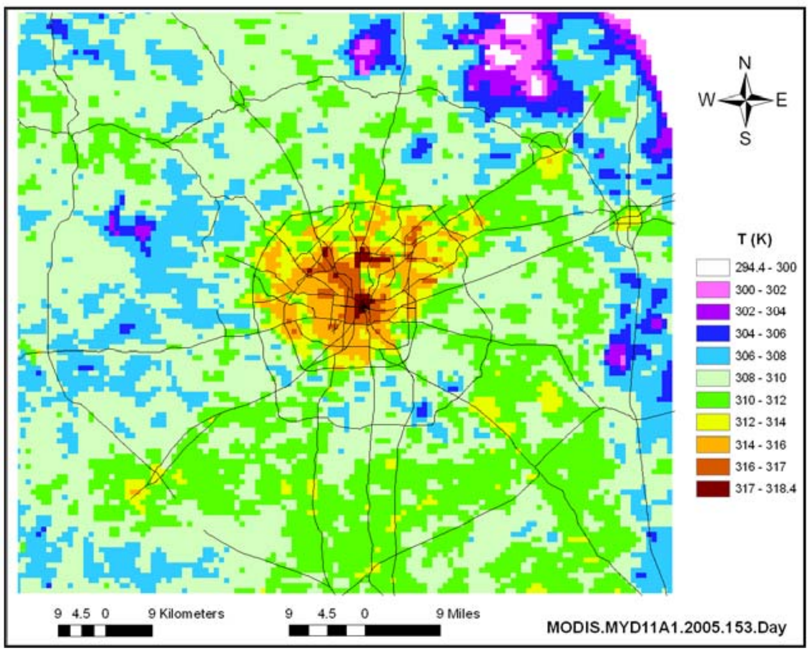

Fig. 4. Daytime (1:30 pm, CST) LST map on 6/2/2005 derived by MODIS/Aqua data. The heat island phenomenon is clearly shown in the downtown area and several other small areas. The four major water bodies (lakes) have lowest temperature.

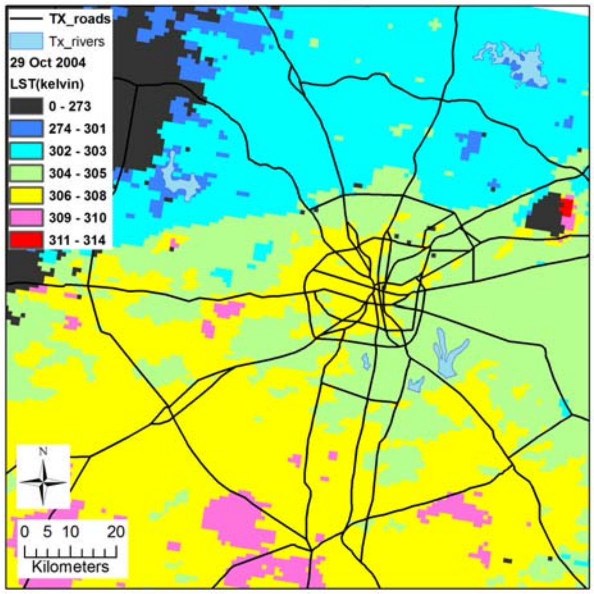

(a) Nov. UHI episode in 2004

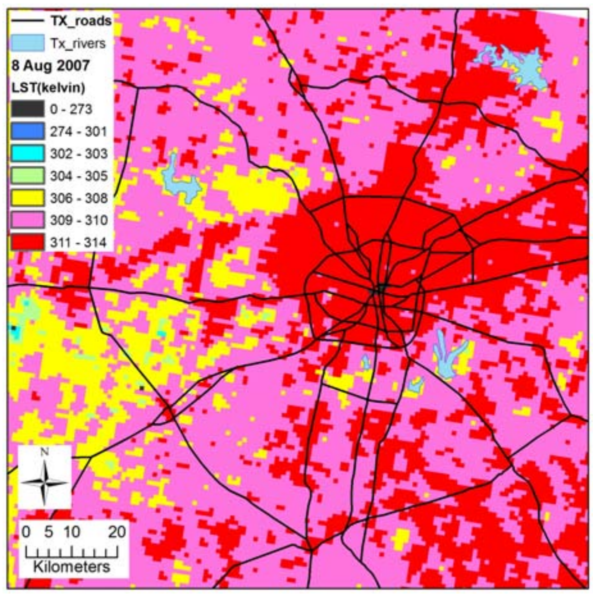

(b) Aug. UHI episode in 2007

Fig. 5. Spatial analyses based on two MODIS LST images**.**

4.2 The Long-term UHI Assessment

We averaged out all available 8-day MODIS temperature products from MODIS/Aqua (1:30 a.m.) for spring/summer seasons, fall/winter seasons, and for all years in the study region to retrieve the spatial trends with differing temporal scales. Figures 6-8 collectively show the mean LST at 1:30 a.m. based on MODIS/Aqua data for spring/summer scenario (Fig. 6), fall/winter scenario (Fig. 7), and scenario of all years (Fig. 8) between 2002 and 2008. On all images, the 4 lakes (water bodies in Fig. 1) had the highest temperature. They were simply due to the high heat capacity of water. Other than that the UHIs revealed very clear patterns seasonally and yearly. On the yearly map (Fig. 8), the UHIs (288-289 °K) were mainly apparent in three areas: the downtown, the intersection area of I10 and Loop 410 northwest, and the San Antonio International Airport. This is similar to the daily map as seen in Fig. 4. However, in the spring/summer scenario (Fig. 6), the central UHI (294-295 °K) was limited to a small downtown area; yet the area with second highest temperature (293-294 °K) was expanded from the downtown to the north, northwest, northeast, and south, resulting in a huge interconnected hot zone. On the fall/winter map (Fig. 7), similar phenomena can be shown in the spring/summer scenario, from which the central small-scale UHI (283-284 °K) was limited to the downtown area, and the second highest temperature (282-283 °K) has similar but less expansive when compared with that in the spring/summer scenario. Nevertheless, it is interesting to find that there is a low temperature zone (safe island) within the second highest temperature area of the fall/winter map. These two small-scale UHIs (intersection area of I10 and Loop 410 northwest and the San Antonio International Airport) appeared on the yearly map, which are deemed as an integral part of the expansive second highest temperature area on the spring/summer map as well as on the fall/winter map.

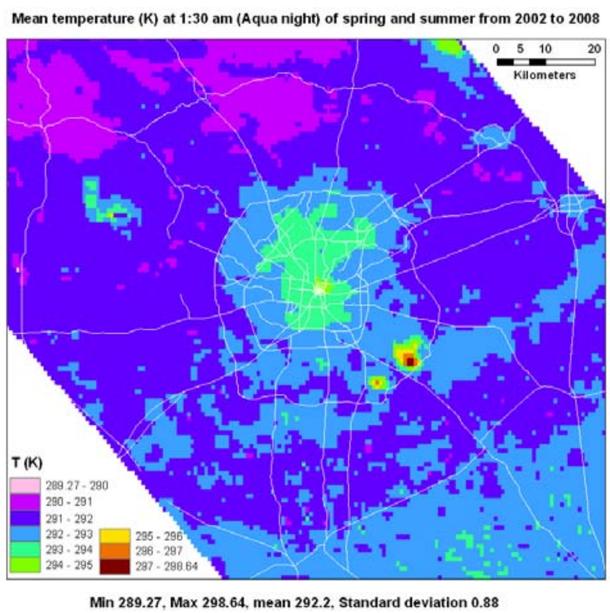

Fig. 6. San Antonio mean LST at 1:30 a.m. based on MODIS/Aqua data in spring and summer between 2002 and 2008.

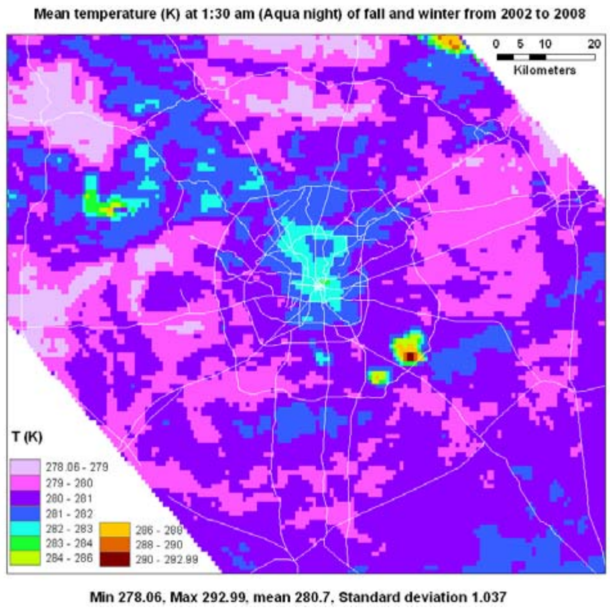

Fig. 7. San Antonio mean LST at 1:30 a.m. based on MODIS/Aqua data in fall and winter between 2002 and 2008.

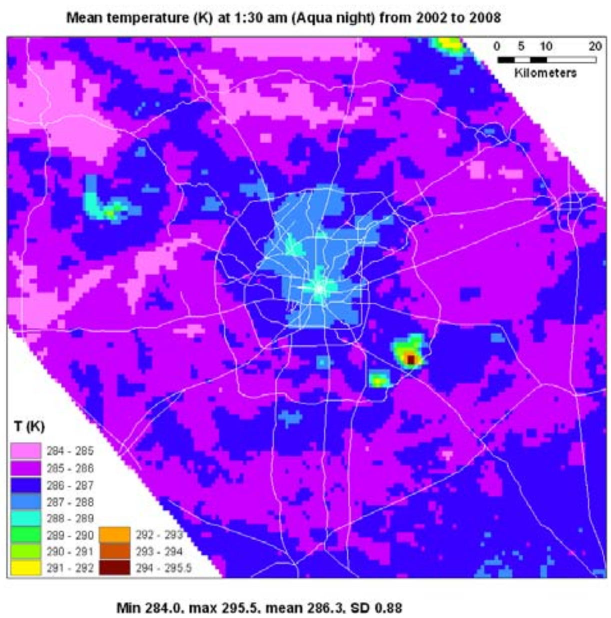

Fig. 8. San Antonio mean LST at 1:30 a.m. based on MODIS/Aqua data between 2002 and 2008.

4.3 Final Remarks of Perspective Future Studies

Two mainstreams of future research associated with the UHIs can be identified and discussed as below. One is related to the interactions between the urban landscape dynamics and the UHIs. These interactions may possibly lead to the examine the effect of urban surface composition and structure on urban surface energy budgets, thereby getting a better understanding of the thermal behavior of urban landscapes. The other is to correlate the UHIs to local weather patterns such as urban storms. Both are important for adaptive management strategies under the umbrella concept of urban sustainability. They can be briefly discussed as follows.

4.3.1 Possible Linkages between UHI and NDVI

Average NDVI of the study area increased from the dry winter to the growing season in the summer due to precipitation, sun light, and temperature changes. The temporal changes of NDVI profiles were presented in Fig. 9 for comparison. In general, higher NDVI might be correlated with decreasing LST depending on the degree of evapotranspiration [22][23]. Gallo et al. [24] used data from the NOAA Advanced Very High Resolution Radiometer (AVHRR) to determine urban/rural differences in surface temperature and vegetation index for 37 U.S. cities. They found that the difference in vegetation index showed a positive correlation with the differences in both surface and air temperature. An advanced analysis on the relationship between LST, NDVI and Shannon Diversity Index (SHDI) was conducted in the City of Shanghai, China [25] and it showed a positive correlation between LST and SHDI and a negative correlation between NDVI and SHDI. As a result, LST, SHDI and NDVI can be considered to be three basic indices to study the urban ecological environment.

By looking into the NDVI maps in Fig. 9, there is a consistent decline in NDVI values with increased level of urban development. No matter where our focal point is placed upon in winter or summer maps, urban NDVI values are always smaller than the rural areas in San Antonio, Texas when compared the NDVI distribution in Fig. 9 against the land use patterns in Fig. 1. Comparison between Fig. 6 and Fig. 9(a) reveals an obviously similar spatial pattern between the spring/summer LST and the spring/summer NDVI. Yet there is no such obvious linkage when comparing Fig. 7 and Fig. 9(b). We believed that such linkages between surface temperature and vegetation index associated with land use and land cover change can contribute to some extent a better urban landscape design to avoid flash flood and achieve energy saving in buildings eventually [26]. Hence, the interannnual changes in vegetation activities using NDVI and its relationships to temperature changes may be examined further in the future.

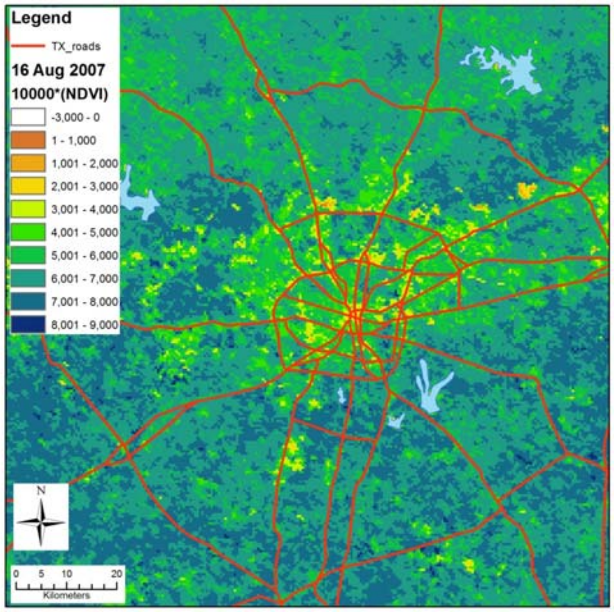

(a) Aug. 16th 2007

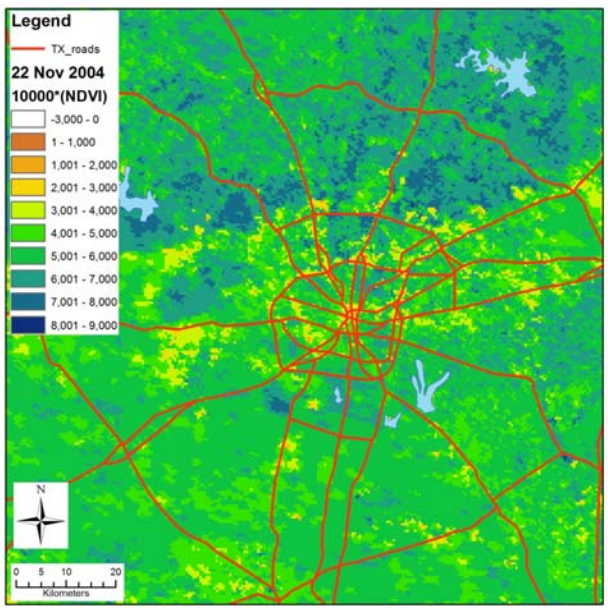

(b) Nov. 22nd 2004

Fig. 9. The NDVI maps in the study area and time periods of interest.

4.3.2 Possible Connections between UHI and Urban Storm Events

According to the rainfall-runoff record within the seven-year time frame, there were three flooding events that occurred in mid 2002, late 2004, and mid-late 2007. They are marked by squared numbers sequentially in Fig. 10. In general, the UHI usually reaches its highest intensity on summer nights**.** In Fig. 10, scenarios 1, 2 and 3 were marked up for the purpose of illustration in this study because these are the biggest storm events in the summer or late summer in 2002, 2005, and 2007. The UHI in San Antonio may be affecting or affected by several hydrometeorological factors along the coastal bend area of Texas. In principle, The UHI may only be connected to convective lifting rather than orographic lifting and frontal cyclone. However, in the case of San Antonio, continental or maritime air masses may encounter along the shoreline and impact the movement of frontal zone simultaneously. Such sea-land contrasts can generate significant horizontal variability in daytime mixing depths, including shallow mixing depths at the coastline. It leads to grow inland with distance from the Texas coastal bend during onshore flow conditions. As evidenced by the simple ratios in Figs. 11(a) and 11(b), surface cooling in the evening might decouple the flow in the upper part of the previous afternoon's mixed layer from surface friction and results in cyclic fluctuations of simple ratios under the meteorological trends at both regional and continental scales. It can be seen that single or multiple storm episodes sometimes follow the big variations of LST as marked by squared numbers in both Figs. 11(a) and 11(b) qualitatively. Obviously, some of the storm events might be triggered by different causes such as frontal cyclone at the continental scale that might not be directly related to the local UHI effect at all. From the 305th to 329th day in 2004, precipitation played a critical role to cool down high LST continuously. Alternatively, the intermittent increase or decrease of LST might be the major cause that triggered multiple storm events at the local scale. From the 193th to 209th day in 2007, multiple storm events quickly cooled down LST followed by a continuous increase of LST that might be the cause that triggered the major storm event in Aug. 2007. Overall, using high-resolution daily satellite imagery and measurements of the optical and thermal properties combined with local micrometeorological models may become a good tool in the future to understand cooling and heating regions leading to reveal internal relationships between atmospheric heat islands and urban surface characteristics [9][27].

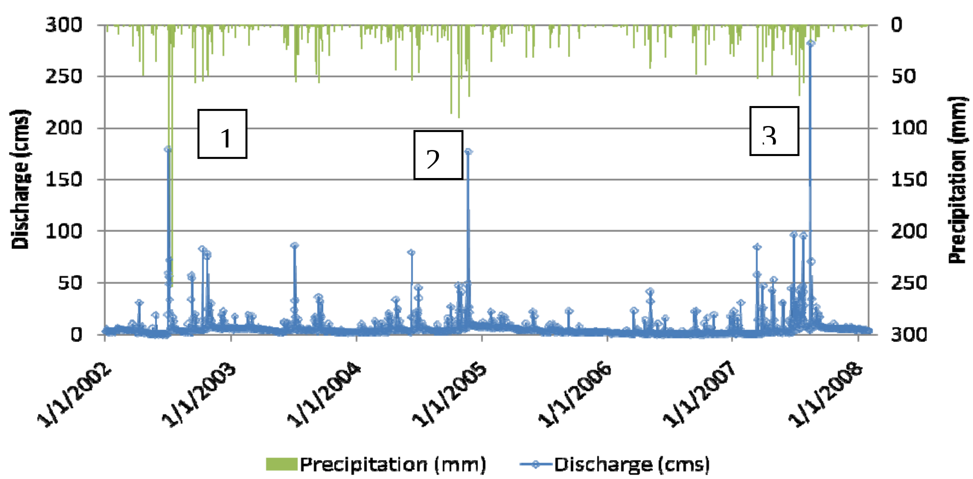

Fig. 10. Summary of time series storm events and discharges in the San Antonio River nearby San Antonio.

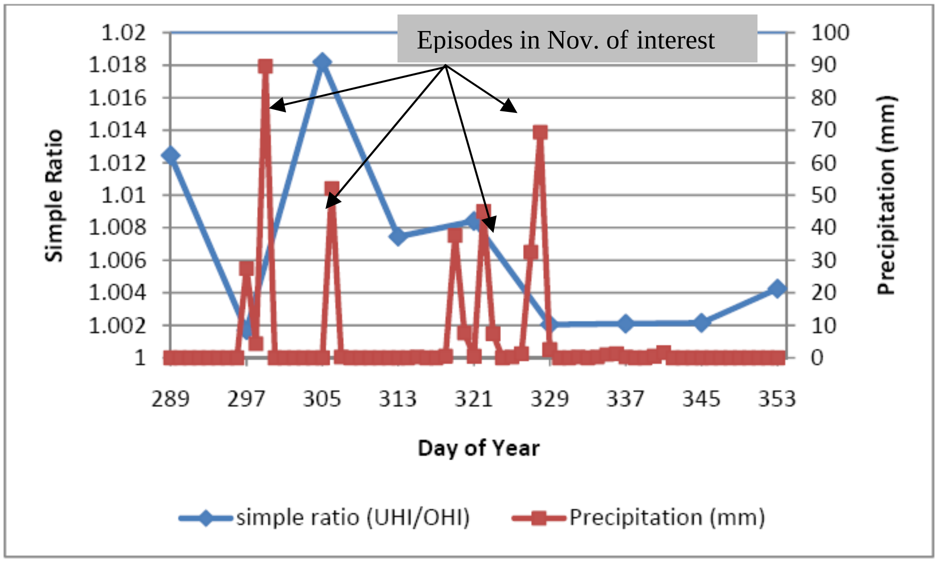

(a) Oct.-Nov. 2004

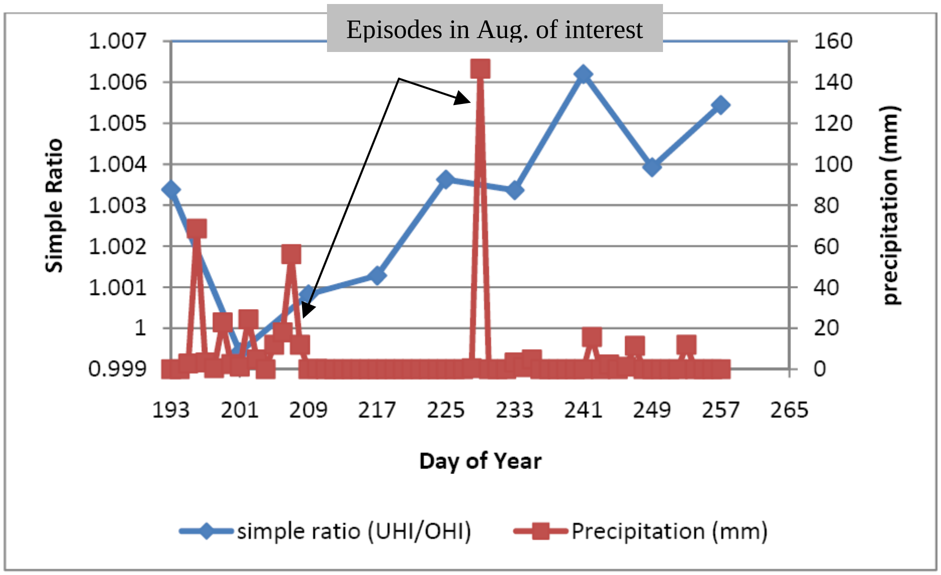

(b) Aug-Sept. 2007

Fig. 11. Temporal correlation analyses between the simple ratios and the storm events.

5 CONCLUSIONS

The UHI is the best-documented example of small-scale anthropogenic climate change and its effect associated with land use and land cover patterns, NDVI variations, and storm events deserve scientific investigation. This study presents the long-term UHI effect of the city of San Antonio located in a semi-arid region - south Texas. With the aid of continuous long-term environmental sensing and monitoring database, it enables us to isolate seasonal variations and overall trends of UHI from 2002 to 2008. The existence of an UHI of the San Antonio downtown area was clearly shown in about 90% of the available cloud-free (or cloudless) data from June 1-September 30 each year. It is especially prevalent in the night-time imagery than in the daytime imagery due to less cloud contamination. During nighttime, the heat island (HI) is about 4 - 5 °K (6 - 8 °F) higher than the average temperature of the study area and 6 - 7 °K (8 - 12 °F) higher than the rural area. Surprisingly, the UHI phenomenon is found not only in the downtown area, but also several other small areas in the northern corner of city's urban area.

We also discussed that the UHI has something to do with urban land use and land cover changes/patterns. Through the change of the surface-energy balance due to land cover modifications, the UHI might be consistent with seasonal trends of NDVI variations to some degree. Within this context, we also presented a preliminary assessment to connect a few urban storm events with the UHI based on a seven-year MODIS/Aqua data and simple ratios. Yet such mild correlation between the UHI and storm events does not imply that local and regional storms can only be induced by the UHIs. But it will be up to other micrometeorologists to explore the micro-scale linkages between the UHI and storm events in the future since heat island may also enhance rainfall caused by orographic uplifting and even frontal systems. Such concern may be related to the changes of urban landscape too resulting in the linkages between land use changes and NDVI variations at the same time. These disturbances could pose indirect impacts to urban sustainability and even human health.

Acknowledgments

This project was partly supported by the UTSA grant of Tenure-Track Research Award Competition (2008-2009). Critical reviews and constructional comments from two anonymous reviewers to improve the quality of this manuscript are greatly appreciated. The provision of data by NASA EOS Data Center and USGS are also sincerely acknowledged.

References

[1] S. Kato and Y. Yamaguchi, "Analysis of urban heat island effect using ASTER and ETM+ data -separation of anthropogenic heat discharge and natural heat radiation in sensible heat flux," *Rem. Sens. Environ.* **99**(1-2), 44-54 (2005) [doi: 10.1016/j.rse.2005.04.026].

[2] Southwest Research Institute (SWRI), Published in the Fall 1997 issue of Technology Today®, (1997) http://www.swri.edu/3pubs/ttoday/fall97/heat.htm**.**

[3] National Aeronautic and Space Administration (NASA) (2000). http://www.gsfc.nasa.gov/topstory/20020613urbanrain.html.

[4] C. Rosenzweig, W. D. Solecki, L. Parshall, M. Chopping, G. Pope, R. Goldberg, "Characterizing the urban heat island in current and future climates in New Jersey," *Global Environ. Change Part B: Environ. Hazards* **6**(1), 51-62 (2005) [doi:10.1016/j.hazards.2004.12.001].

[5] F. Yan, Z. Qin, and Y. Wang "Application of MODIS data to assess the urban heat island in Shanghai City, China," *Proc SPIE* **6752**, 67521T (2007) [doi: 10.1117/12.760707].

[6] A. Chudnovsky, E. Ben-Dor, and H. Saaroni, "Diurnal thermal behavior of selected urban objects using remote sensing measurements," *Energy Build.* **36**, 1063-1074 (2004) [doi: 10.1016/j.enbuild.2004.01.052].

[7] B. D. Katsoulis and G. A. Theoharatos, "Indications of the urban heat island in Athens, Greece," *J. Climate Appl. Meteorol.* **24**, 1296-1302 (1985) [doi:10.1175/1520-0450(1985)024<1296:IOTUHI>2.0.CO;2].

[8] T. R. Oke, *Initial Guidance to Obtain Representative Meteorological Observations at Urban Sites*, Instruments and Observing Methods Report No. 81, World Meteorological Organization (WMO),

http://www.wmo.ch/pages/prog/www/IMOP/publications/IOM-81/IOM-81-UrbanMetObs.pdf.

[9] Th. Nitis, Z. B. Klaic, D. Kitsiou, and N. Moussiopoulos, "Meteorological simulations with use of satellite data for assessing urban heat island under summertime anticyclonic conditions," *Int. J. Environ. Pollut*. **40**, 123-135 (2010) [doi: 10.1504/IJEP.2010.030888].

[10] J. A. Voogt and T. R. Oke, "Thermal remote sensing of urban climates," *Rem. Sens. Environ.* **86**, 370-384 (2003) [doi: 10.1016/S0034-4257(03)00079-8].

[11] G. Rigo and E. Parlow, "Modelling the ground heat flux of an urban area using remote sensing data," *Theor. Appl. Climatol*. **90**, 185-199 (2007) [doi: 10.1007/s00704-006-0279-8].

[12] D. R. Streutker, "Satellite-measured growth of the urban heat island of Houston, Texas," *Rem. Sens. Environ.* **85**(3), 282–289 (2003) [doi: 10.1016/S0034-4257(03)00007-5].

[13] D. O. Lee, "Urban warming?: an analysis of recent trends in London’s heat island," *Weather* **47**, 50-56 (1992).

[14] Q. Weng, D. Lu, and J. Schubring, "Estimation of land surface temperature-vegetation abundance relationship for urban heat island studies," *Rem. Sens. Environ.* **89**(4), 467-483 (2004) [doi: 10.1016/j.rse.2003.11.005].

[15] National Oceanographic and Atmospheric Administration (NOAA), *Final Rapid Science Synthesis Report: Findings from the Second Texas Air Quality Study* (2007) http://www.esrl.noaa.gov/csd/2006/rss/rsstfinalreport083107.pdf.

[16] United States Geological Survey (USGS), *National Water Information System* (2008a), http://waterdata.usgs.gov/nwis

[17] National Aeronautic and Space Administration, *Warehouse Inventory Search Tool* (2008) http://wist.echo.nasa.gov/~wist/api/imswelcome/.

[18] Z. Wan, Y. Zhang, Q. Zhang, and Z. L. Li, "Quality assessment and validation of the MODIS global land surface temperature," *Int. J. Remote Sens.* **25**, 261-274 (2004a) [doi: 10.1080/0143116031000116417].

[19] Z. Wan, P. Wang, and X. Li, "Using MODIS land surface temperature and normalized difference vegetation index for monitoring drought in the southern Great Plains, USA," *Int. J. Remote Sens.* **25**, 61-72 (2004b) [doi: 10.1080/0143116031000115328].

[20] United States Geological Survey (USGS) (2008) https://lpdaac.usgs.gov/lpdaac/tools/modis_reprojection_tool.

[21] M. Momeni, and M. R. Saradjian, "Evaluating NDVI-based emissivities of MODIS bands 31 and 32 using emissivities derived by Day/Night LST algorithm," *Rem. Sens. Environ.* **106**(2), 190-198 (2007) [doi:10.1016/j.rse.2006.08.005].

[22] A. Higuchi, T. Hiyama, Y. Fukuta, R. Suzuki, and Y. Fukushima, "The behaviour of a surface temperature/vegetation index (TVX) matrix derived from 10-day composite AVHRR images over monsoon Asia," *Hydrolog. Process.* **21**(9), 1157-1166 (2007) [doi: 10.1002/hyp.6676].

[23] M. Stathopoulo, A. Synnefa, C. Cartalis, M. Santamouris, T. Karlessi, and H. Akbari, "A surface heat island study of Athens using high-resolution satellite imagery and measurements of the optical and thermal properties of commonly used building and paving materials," *Int. J. Sustain. Energy* **28**(1), 59-76 (2009) [doi: 10.1080/14786450802452753].

[24] K. P. Gallo, A. L. Mcnab, T. R. Karl, J. F. Brown, J. J. Hood, and J. D. Tarpley, "The use of NOAA AVHRR data for assessment of the urban heat-island effect." *Int. J. Rem. Sens.* **14**, 2223-2230 (1993) [doi:10.1080/01431169308954031].

[25] W. Yue and W. Tan, "The relationship between land surface temperature and NDVI with remote sensing: application to Shanghai Landsat 7 ETM+ data," *Int. J. Rem. Sens.* **28**(15), 3205-3226 (2007) [doi: 10.1080/01431160500306906].

[26] E. F. Lambin and D. Ehrlich, "The surface temperature-vegetation index space for land-cover and land-cover change analysis," *Int. J. Rem. Sens.* **17**(3), 463-487 (1996) [doi:10.1080/01431169608949021].

[27] W. L. Stefanov and A. J. Brazel, "Challenges in characterizing and mitigating urban heat sslands — a role for integrated approaches including remote sensing," *Applied Remote Sensing for Urban Planning, Governance and Sustainability*, M. Netzband, W. L. Stefanov, and C. Redman, Eds., Springer Berlin Heidelberg, (2007) [doi: 10.1007/978-3-540-68009-3_6].